Water Science and Engineering 2023, 16(3): 261–270

HOSTED BY

ELSEVIER

Available online at www.sciencedirect.com

Water Science and Engineering

journal homepage: wse.hhu.edu.cn

Insights into remediation technology for malachite green wastewater treatment

Peter Olusakin Oladoye [a,b,*], Timothy Oladiran Ajiboye [c,d], Wycliffe Chisutia Wanyonyi [e], Elizabeth Oyinkansola Omotola [f], Mayowa Ezekiel Oladipo [a]

[a] *Department of Chemistry and Biochemistry, Florida International University, Miami 33199, USA*

[b] *Analytical/Environmental Chemistry Unit, Department of Pure and Applied Chemistry, Ladoke Akintola University of Technology, Ogbomoso 210214, Nigeria*

[c] *Department of Chemistry, Nelson Mandela University, Summerstrand 6031, South Africa*

[d] *Material Science Innovation and Modelling (MaSIM) Research Focus Area, Faculty of Natural and Agricultural Sciences, North-West University, Mmabatho 2735, South Africa*

[e] *Department of Mathematics, Actuarial and Physical Sciences, School of Science and Technology, University of Kabianga, Kericho 20201, Kenya*

[f] *Department of Chemical Sciences, Tai Solarin University of Education, Ijebu Ode 120101, Nigeria*

Received 2 October 2022; accepted 6 March 2023

Available online 16 March 2023

Abstract

Malachite green (MG) dye is a common industrial dye and organic contaminant that can be found in (waste)water. Textile and food industries make use of MG as dyeing and food coloring agents, respectively. However, MG is both genotoxic and mutagenic. Hence, the elimination of MG from MG-laden-wastewater is germane. This review summarizes up-to-date researches that have been reported in literature as regards the decontamination of toxic MG wastewater. Various removal methods (adsorption, membrane, Fenton system, and heterogenous and homogeneous photodegradation) were discussed. Of the two basic technologies that are comprehensively explored and reviewed, chemical treatment methods are not as viable as physical removal methods, such as the adsorption technology, due to the lack of secondary pollutant production, simple design, low operation costs, and resource availability. This review also presents various practical knowledge gaps needed for large-scale applications of adsorptive removal methods for MG. It concludes by recommending further research on the techniques of cheap and simple decontamination of MG to get clean water.

Keywords: Contaminant; Wastewater; Decontamination; Pollution; Malachite green; Dye

1. Introduction

About 29% of the total world population, amounting to 2.1 billion people, needs access to securely managed water while 11% requires access to better-quality water services within a 30-min walking distance from their households (Chen et al., 2007; WHO, 2017). Also, there are many people that dwell in poor-quality water environments due to the lack of sanitation and excess flooding (Young et al., 2019). This causes water quality insecurity for lives of humans and animals. It has been projected that about 5 billion of the global population would experience water scarcity and water pollution challenges by the year 2050, with South Asia and Sub-Saharan Africa greatly negatively impacted (Chaplin-Kramer et al., 2019; Oladoye et al., 2022). In urban setting, industrial wastewater is one of the prominent sources of surface and ground water contamination. For instance, pulp and paper, textile, smelting, food, and pharmaceutical industries generate both organic and inorganic pollutant-loaded wastewater.

The dyeing and textile industries release a large magnitude of wastewater with many non-biodegradable and biodegradable contaminants (Pandey et al., 2022). Although textile/dyeing

* Corresponding author.
E-mail address: poladoye@fiu.edu (Peter Olusakin Oladoye).
Peer review under responsibility of Hohai University.

https://doi.org/10.1016/j.wse.2023.03.002

wastewater consists of a number of contaminants, synthetic coloring dyes are of concern because a large volume of them is used while a very small amount binds to fabric and the rest is discharged as effluent. Globally, a total of 3×10^8 kg of dyes are discharged as wastewater on an annual basis (Sghaier et al., 2019). Textile industries alone are responsible for releasing a high magnitude of polluted wastewater. Annually, about 6.40×10^8 m^3 and 1.84×10^9 m^3 of wastewater are discharged in India and China, respectively (Kishor et al., 2021; Samuchiwal et al., 2021).

Among various forms of dye that are used in product manufacturing, malachite green (MG) dye must be reckoned with. The physico-chemical properties of MG dye are presented in Table 1. It has been used as dye for leather, jute, cotton, paper, silk, and wool, and as food coloring additive (Srivastava et al., 2004; Amuda et al., 2007). In addition, MG can also be used in aquaculture as antiseptic and fungicide, as well as medical anthelminthic and disinfecting agent (Chen et al., 2007). However, due to the persistence and bioaccumulation tendency of MG dye, it accumulates in aquatic animals when it is discharged in the water body, and it eventually enters into the human system via the food chain (Shi et al., 2018; Shrivastava et al., 2022). MG exhibits various forms of associated potential toxic effects like carcinogenesis, teratogenesis, and mutagenesis in the human body (Lellis et al., 2019; Song et al., 2020). Furthermore, in the mammalian body system, MG can be biochemically reduced to a chemical substance known as leucomalachite (LMG) (Fig. 1) that can accrue in the body for greater than five months (Oplatowska et al., 2011). LMG has been found to increase lung adenomas in F344 male rates, facilitating liver tumor when appropriately initiated (Culp et al., 2002).

Consequently, it is imperative that proper and/or effective wastewater treatment be carried out prior to the discharge of MG dye-containing wastewater into the environment.

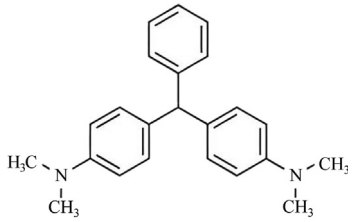

Fig. 1. Molecular structure of leucomalachite.

Currently, there are a number of treatment technologies or strategies for the remediation of wastewater contaminated with MG dye. Some strategies adopted for removing MG depend on the operational treatment cost, waste product composition, and the dye's nature (Raval et al., 2022). These methods are categorized into physical and chemical technologies (Wu et al., 2022). The techniques involved in each of the methods are summarized in Fig. 2. A number of compilation of studies on the aforementioned treatment methods have been published but with inherent gaps to be filled, such as the lack of specificity for a particular dye and consideration of a single method of treatment (El-Kady et al., 2018; Dihom et al., 2022). These published reviews, however, only presented individual methods and thus, lacked comparisons of methods, as well as details on the practical-knowledge gap regarding the adsorption technology.

However, this review presents a synthesis of various studies on physical and chemical treatment strategies for MG dye. It comprehensively and extensively explores, describes, and highlights the differences (merits and demerits inclusive) of the two main MG dye wastewater treatment strategies. Owing to the low-cost and ease of design of adsorption technologies, the review specially enumerates and discusses various factors for adsorptive removal methods of MG dye for the effective design of wastewater treatment plants.

Table 1
Physicochemical properties of MG dye.

Common name	Molecular formula	Molecular formula weight (g/mol)	IUPAC name	Other known name	Molecular structural formula
Malachite oxalate	$C_{52}H_{54}N_4O_{12}$	927.000	[4-[[4-(Dimethylamino)phenyl]-phenylmethylidene]cyclohexa-2,5-dien-1-ylidene]-dimethylazanium; 2-hydroxy-2-oxoacetate; oxalic acid	Aniline green; basic green 4; diamond green B; Victoria green B	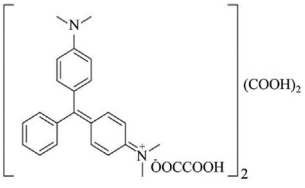
Malachite chloride	$C_{23}H_{25}ClN$	364.911	[4-[[4-(Dimethylamino)phenyl]-phenylmethylidene]cyclohexa-2,5-dien-1-ylidene]-dimethylazanium; chloride		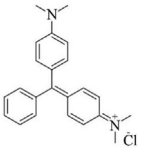

Note: IUPAC refers to the International Union of Pure and Applied Chemistry.

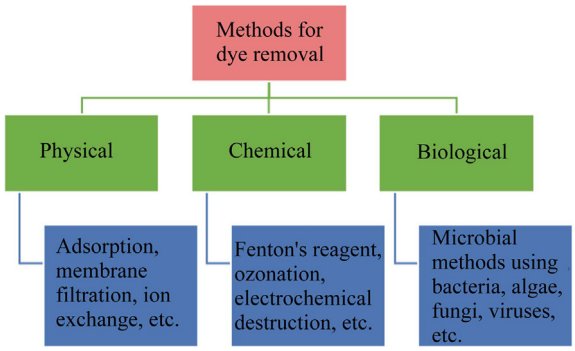

Fig. 2. Methods employed for removal of dye from environment.

2. Removal strategies for malachite green dye

2.1. Physical removal methods

2.1.1. Adsorption technology

The adsorption technology is the most common method that has been reported for the removal of dye (Ho, 2020). Usually, this method involves the synthesis of appropriate adsorbents, which is followed by the characterization of the material using various physicochemical techniques (Moradi and Panahandeh, 2022). These characterization procedures include phase identification of the material, provision of information on unit cell dimensions, and identification of the presence of organic and inorganic compounds in the material (Sleeman and Carter, 2005; Patel et al., 2021). The specific functional groups prevalent in the material are determined via spectrum data (Mohamed Shameer and Mohamed Nishath, 2019). They also produce images that reveal the morphology and composition of the surface of materials (Hubbs et al., 2013; Zhao and Liu, 2022). Once the characterization steps confirm the prowess of materials to remove the dye, appropriate procedures are carried out to achieve the purpose for which the material was synthesized. These include the alterations of pH, dosage, contact time, temperature, and the concentration of the dye (Tran et al., 2022). Examples of various adsorbents that have been used in the removal of MG are summarized and presented in Table A.1 in Appendix A.

Based on the surveyed literature presented in Table A.1, the adsorbent removal efficiency ranged from 78.88% with sulfur-doped titanium dioxide (S-TiO_2) (Giang et al., 2022) to 99.86% with sulfur-doped titanium dioxide/porous reduced graphene oxide (S-TiO_2/rGO) (Giang et al., 2022). Furthermore, green adsorbents (eco-friendly) have been used to achieve a similar purpose. This includes crab shell biochar (Wu et al., 2022), *Zingiber officinale* plant leaves (Buvaneswari and Singanan, 2022), laccase immobilized biochar (pine needle) (Pandey et al., 2022), and rice husk-modified biochar (Tsai et al., 2022). The removal efficiencies of these green adsorbents were 99%, 88%, greater than 85%, and 95%, respectively. Moreover, non-green materials that are purely synthesized but prepared using green materials have also been used. This comprises watermelon rind-styrene-based molecular imprinted polymer (Awokoya et al., 2022) and green iron–copper oxides, which are synthesized using *Parthenocissus quinquefolia* (Zhang et al., 2018). Sometimes, the adsorption process is combined with a bioremediation process (phycoremediation), as seen in a recently published article (Pathy et al., 2022). Pathy et al. (2022) employed the microalgal-kombucha-SCOBY (symbiotic culture of bacteria and yeast) composite to remove MG from aqueous solutions and achieved a removal efficiency greater than 98%, indicating the efficacy of the combined technique in treating MG-loaded wastewater.

2.1.2. Membrane technology

Another effective method, through which dye can be removed from aqueous media, is membrane processes (Marszałek and Żyłła, 2021). Membrane is a specific permeable medium or barrier that has the ability to restrict the movement of certain materials of different sizes (Ahmad et al., 2002). Precisely, the term concerning this process is the membrane filtration process. This process can be operated using two main approaches, which are the cross-flow and dead-end filtration, depending on the direction of the feed stream to the orientation of the membrane (Scott et al., 1996). Based on the two approaches of membrane filtration, the process is generally achieved via any of the four methods (Allègre et al., 2006; Kumar et al., 2012) shown in Fig. 3.

However, a significant fall-out is associated with the use of the membrane filtration process, which is the clogging of the filter pores by dye molecules. This challenge makes the membrane process less utilized in the dye industry for wastewater treatment (Kumar et al., 2012). Consequently, filters are continuously changed to achieve high dye removal efficiencies. This process makes the membrane method uneconomical due to its high cost and short life span (Kumar et al., 2012). Perhaps this disadvantage is why research works have not focused on using membrane technologies to remove MG from the environment. Of all the scientific articles considered in this study, only two research works reported the removal of MG from aqueous solutions using the membrane technique. Raval et al. (2022) employed an emulsion liquid membrane, while Iqbal et al. (2022) used the cross-flow membrane filtration (Iqbal et al., 2022) with removal efficiencies of 94.99% and 97.00%. Apparently, the use of membrane technologies for removing

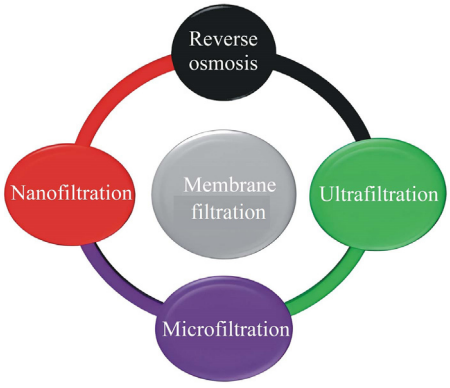

Fig. 3. Membrane filtration processes used for removal of dyes.

MG from the environment should be fully explored, even though they show prospects concerning the removal of MG. It therefore requires that this method should be investigated more closely and might be combined with other techniques to ensure a 100% removal efficiency of MG, provided that it is non-toxic.

2.2. Chemical removal methods (photochemical and non-photochemical methods)

2.2.1. Non-photochemical methods

2.2.1.1. Fenton system for degrading malachite green. The reagents of Fenton are made from hydrogen peroxide and divalent iron (Ajiboye et al., 2020). The reaction of these two materials leads to the generation of hydroxyl radicals that are highly oxidizing:

$$Fe^{3+} + H_2O_2 \rightarrow Fe^{3+} + \cdot OH + OH^- \quad (1)$$

Hydroxyl radicals attack MG molecules to generate products that are either non-toxic or less toxic. Hashemian (2013) used the Fenton process to degrade 95.5% of MG within 15 min under acidic conditions. It was observed that the Fenton degradation of MG was an endothermic process and could be described by the pseudo-second-order kinetic model. With 20 mg/L of MG, an initial divalent iron concentration of 0.10 mmol/L, and an initial hydrogen peroxide (H_2O_2) concentration of 0.50 mmol/L, there was 99.25% degradation of MG within 1 h. The reaction was, however, carried out at a constant temperature of 30°C under acidic conditions (Hameed and Lee, 2009). In another investigation by Chen et al. (2002), the Fenton process catalyzed with different aromatic organic additives was used to degrade MG. The presence of the aromatic organic content sped up the MG degradation rate and revealed the effect of the addition of amido aromatics, carboxylic aromatics, *p*-benzoquinone, *m*-hydroxylbenzoic acid, *p*-hydroxylbenzoic acid, salicylic acid, and hydroquinone. Hydroquinone had the greatest impact on the rate of the degradation of MG. This is because it has the ability to continuously regenerate Fenton reagents. Complexes have also been used to catalyze the Fenton reaction for the degradation of MG. For example, [Fe(III)-salen]Cl complex displayed 97.94% decolorization and 54.35% total organic carbon removal within 24 min when it was introduced into the Fenton system (Bai et al., 2013). Several modified forms of the Fenton process have been used to remove MG dye, and some of them are shown in Table 2.

2.2.2. Photochemical methods

2.2.2.1. Ultraviolet (UV) light-assisted advanced oxidation process. UV light has been utilized in combination with other reactive species to affect the degradation of MG. Generally, the UV light-assisted oxidation process, otherwise known as homogenous photodegradation, is advantageous because there is no formation of sludge and it is usually carried out under ambient temperatures (Modirshahla and Behnajady, 2006; Ghodbane and Hamdaoui, 2010). One of the combinations is the use of ordinary hydrogen peroxide with UV light. The widely accepted mechanism for their reaction is the splitting of hydrogen peroxide in the presence of UV light to generate hydroxyl radicals. The generated hydroxyl radicals then attack MG molecules (and other organic pollutants) to produce other highly reactive organic radicals that lead to complete oxidative degradation of the dye (Modirshahla and Behnajady, 2006). Another form involves the combination of UV light with ferrous ions and hydrogen peroxide. This combination has particularly been reported to be better than the use of UV/H_2O_2. The effectiveness of the UV/H_2O_2/Fe^{2+} process is influenced by the concentration of ferrous ions (Khan et al., 2013). In an investigation where 60 mg/L of ferrous ion was used, there was 98% MG molecule degradation within 1 h under acidic conditions, but there was 94% MG molecule decomposition without the introduction of ferrous ions (Ghime et al., 2019). Although UV is good for homogenous photodegradation, other forms of light have been investigated as a replacement for UV light. Homogenous photodegradation of MG molecules has been reported with good results. For instance, pulsed light was used in combination with hydrogen peroxide to degrade MG molecules. Complete decolorization of the dye was observed with the use of 75-J/cm^2 pulse light, and the rate of degradation was found to be 0.071 0 cm^2/J (Navarro et al., 2019).

2.2.2.2. Catalyst-assisted advanced oxidation process. Photocatalysts are semi-conductors that are sensitive to light due to the fact that they possess band gap. They absorb photons, which causes the excitation of electrons from the valence band to the conduction band as much as the absorbed photon energy is either equal to or greater than the band gap energy. The excitation of electrons causes the positively charged holes to be released in the valence band of the semiconductors. However, there is feasibility of the photo-generated electrons (e^-) and holes (h^+) to recombine, thereby leading to the release of heat energy. On the other hand, the two reactive species may undergo further reactions to generate other highly oxidizing species that are useful for the degradation of organic pollutants. For instance, holes can react with water to generate highly oxidizing hydroxyl radicals (·OH) while electrons can react with oxygen to form superoxide radicals (O_2^-). These highly oxidizing species will in-turn attack MG molecules to be less toxic or non-toxic species (Ajiboye et al., 2021b, 2021c; Cheng et al., 2022). The entire process was summarized by Ajiboye et al. (2021a). One of the common photocatalysts that has been used to degrade dyes is titanium oxide nanoparticles (Bharati et al., 2017). To enhance its performance, several modifications have been adopted on titanium oxide nanoparticles. For instance, iron, sodium, and nitrogen were used to modify titanium oxide nanoparticles for better performance. The combination of the impregnation method and green synthesis was used for the modification. It was observed that there was 96.57% degradation of MG molecules within 25.83 min of visible light irradiation (Amigun et al., 2022). As revealed by the machine learning modeling, the optimized conditions for the removal of MG molecules in the presence of the bismuth

Table 2
Various modified Fenton processes used to remove MG dye.

Type of Fenton system	Initial MG concentration	Other conditions	MG degradation performance	Reference
Electro-Fenton	0.5 mmol/L	Room temperature; pH of 3; 0.2 mmol/L of Fe(III)	A pseudo-first-order decay constant of 0.244 min^{-1}	Oturan et al. (2008)
Fenton-like	50 mg/L	pH of 3; H_2O_2 (30%); 1.0×10^{-4} mol/L of Fe(III)	95.5% degradation	Hashemian (2013)
Heterogeneous electro -Fenton and UVA photoelectro-Fenton	50 mg/L	pH of 3.0; 21.7 mA/cm^2	98% mineralization	García-Rodríguez et al. (2016)
Solar-Fenton	3.5×10^{-5} mol/L	pH of 6.75; presence of Fe^0-activated carbon	A pseudo-first-order rate constant of 9×10^{-2} s^{-1}	Singh et al. (2014)
Photo-Fenton	20 mg/L	500-W Xe lamp; neutral pH; 90 mmol/L of H_2O_2	99.9% degradation	Jiang et al. (2018)
Bio-Fenton	20 mg/L	Presence of glucose oxidase; 120 min	78% decolorization	Karimi et al. (2012)

ferrite photocatalyst are pH of 7, a dye concentration of 5 mg/L, a catalyst loading of 1.5 g/L, and a light intensity of 105 W (Jaffari et al., 2022). Other examples of the investigations that utilized photocatalysis for the degradation of MG molecules are shown in Table A.2 in Appendix A.

3. Effects of parameters on adsorption of malachite green dye

Assessment of the reviewed MG removal methods has revealed their demerits. For example, chemical degradation of MG could result in toxic intermediates, and chemical removal methods might result in the release of more chemicals into the MG-treated water. Hence, they are not green approaches. Membrane fouling and high sludge production are characterized with the membrane technology. However, the adsorption technology has few demerits, is of low price, and has attracted many researchers. In order to apply adsorption for large-scale wastewater remediation purposes, it is germane to understand the influence of fundamental operating parameters, such pH, initial MG concentration, dosage, and temperature.

3.1. Influence of solution pH

Solution pH plays a crucial role in influencing the adsorption of MG because it alters the ion mobility, adsorbent surface, and the ionization of MG dye molecules in solutions. The MG structure shows the presence of positive nitrogen ions that makes it a cationic basic dye. On dissolution, oxalate ions in its structure enable the dye to have overall positive charges. At low pH values, the ionic competition between H^+ and MG^+ zwitterion exists in the aqueous solution, reducing the amount of the adsorbed MG. At higher pH values, a higher quantity of MG is adsorbed because the excess of hydroxyl ions limits the competition of H^+ and MG^+, leading to a higher aggregate of MG^+ (Ojediran et al., 2021). Likewise, the MG adsorption capacity and removal percentage decreased in the acidic medium because of the electrostatic repulsion between the cationic MG dye and positively charged adsorbent surface. However, the electrostatic attraction between the negatively charged adsorbent surface and cationic MG dye occurs in the basic solution pH, which increases the MG adsorption capacity and removal percentage.

Few studies have investigated the relationship of the adsorption capacity of MG with different adsorbents in the solution pH range. To evaluate the impact of solution pH on the adsorption of MG, Ramaraju et al. (2014) used rice husk treated with nitric acid and peroxide to adsorb MG from the aqueous solution in a pH range of 2−11 and found an increase in the removal efficiency of MG when the solution pH was increased. The adsorbent surface reacts with hydrogen ions (H^+) at low pH values to form positively charged complex ions ($C-OH_2^+$), which repels MG cations for adsorption and leads to a decreased adsorptive removal of MG. In contrast, the surface of the adsorbent becomes negatively charged ($C-O^-$) at high pH values due to the presence of excess OH^-, thereby promoting the adsorption of the cationic MG dye. The same applies to MG dye removal by activated serpentine mineral decorated with magnetic nanoparticles (MNP/SP). Seliem et al. (2020) studied the influence of pH (2−10) on the MG dye uptake. They found that at acidic pH values, the functional groups of MNP/SP became protonated as $-OH_2^+$ and $Si-OH^+$ that repelled the cationic MG dye for the adsorption site, resulting in decreased MG uptake (Seliem et al., 2020). In contrast, at high pH values, the adsorption process was favorable due to electrostatic interactions between deprotonated groups and the cationic MG dye:

$$MNP/SP^- + C_{23}H_{25}N_2^+ \rightarrow MNP/SP + C_{23}H_{25}N_2 \quad (2)$$

Lee et al. (2011) examined the impact of solution pH on the adsorption of MG using aminopropyl functionalized magnesium phyllosilicate (AMP clay) to remove MG dye in a pH range of 3−10. The result showed that the AMP clay increased the removal rate of MG as pH was increased. In acidic conditions, excess hydrogen ions enhanced the degree of protonation of AMP clay sheets, causing MG to show cationic properties and further leading to a decreased MG removal rate (Oladoye, 2022). The electrostatic force of attraction occurred between the positively charged MG and negatively charged surface of O^- AMP clay sheets, causing the OH side of carbinol base MG to predominantly interact at the neutral amine group of the AMP clay via hydrogen bonding and

leading to a high MG removal rate (Lee et al., 2011). Naushad et al. (2019) also investigated the effect of pH on MG adsorption by para-aminobenzoic acid modified activated carbon (PABA@AC composite) with an initial dye concentration of 15 mg/L, an adsorbent dosage of 30 mg, an agitation speed of 100 r/min, a temperature of 298 K, a time period of 24 h, and a varying pH range of 2−9. The finding indicated that the adsorption of MG increased as pH was increased from 2 to 7 and decreased slightly when pH exceeded 7. At low pH values, the excess of hydronium ions (H_3O^+) led to the protonation of the surface of the PABA@AC composite, which provided high positive charge densities on the PABA@AC composite surface site, thereby decreasing the adsorption of MG cations via electrostatic repulsion. As the solution pH was increased, the surface of the PABA@AC composite became negatively charged, enabling the adsorption of MG on the PABA@AC composite through electrostatic and π−π interactions (Mazloom et al., 2016).

The point of zero charge (pH_{pzc}) of the adsorbent and the degree of acidity (pKa) of MG dye have been used to interpret the adsorption performance of an adsorbent in relation to pH. When pH < pKa, MG exists in anionic form. When pH > pKa, MG exists in cationic form. When pH < pH_{pzc}, the adsorbent surface becomes positively charged, hindering the adsorption of cationic MG dye. In contrast, when pH > pH_{pzc}, the adsorbent surface becomes negatively charged, favoring the adsorption of cationic MG dye molecules. Gündüz and Bayrak (2017) reported the adsorption of MG dye onto the carbonized pomegranate peel (CPP) and depicted the pH_{pzc} value of CPP as 8.65 and the pKa value of MG as 6.9. This means that MG dye was anionic at pH < 6.9, and the adsorbent was cationic at pH < 8.65. At pH < 6.9, MG was anionic, and CPP was cationic, in which the removal rate increased because of the electrostatic attraction between MG and CPP. At pH > 6.9, both MG and CPP were cationic, in which the MG dye uptake remained constant due to van der Waals interaction in the pH range of 7−8. When pH > 8.65, MG was cationic, and CPP was anionic, increasing the adsorption rate due to the combined effects of ionic and van der Waals interactions.

In an aqueous environment, many pollutants are present, including MG. Thus, it is essential to explore the influence of solution pH on MG adsorption in the mixture of dyes. Li et al. (2022) used the anionic methyl orange (MO) dye and cationic malachite green (MG) dye as the model dyes, and the modified attapulgite-reduced graphene oxide composite aerogel (ATP-RGO CA) was used to test the effect of pH. They revealed an improved removal rate of MG by ATP-RGO CA in the binary dye system at pH < 4, compared to the removal rate of MG in the unitary system. At pH > 6, the removal rate of MG by ATP-RGO CA remained constant, which showed that the coexistence of MG and MO significantly promoted the adsorption of MG onto ATP-RGO CA in an acidic environment. Likewise, the adsorption studies of MG, methyl violet, and methylene blue using the amylopectin dialdehyde-Schiff base (APDA-EA) revealed increased dye removal capacities of APDA-EA from pH of 2 to pH of 5.5. A further increase in the solution pH did not alter the dye removal capacity. This could be attributed to that most of the hydroxyl groups of APDA-EA were available for adsorbing these cationic dyes at pH of 5.5, and the MG removal capacity was greater than the other two dyes (Sasmal et al., 2020). In contrast, a study of the dependence of Congo red and malachite green adsorption on the initial solution pH using the ackee apple seed-bentonite composite (CBAAS) observed a different trend. The results revealed that the MG removal capacity slightly decreased from 90% to 84% when pH was increased from 2 to 10, showing that the adsorption mechanism is controlled by electrostatic attraction at low pH values. As pH is increased, the mechanism of adsorption is controlled by π−π interaction or van der Waal's interaction, leading to an insignificant effect of pH on the adsorption capacity (Adebayo et al., 2020). All the reported studies shown in Tables A.3 through A.5 in Appendix A had pH values ranging from 4 to 10. In summary, to ensure a high removal of MG from aqueous solutions with adsorption, the optimum solution pH must be within 4−10, and at these pH intervals, the electrostatic attraction occurs between the cationic MG dye and negatively charged adsorbent.

3.2. Influence of adsorbent dosage

To determine the efficacy of the adsorbent in removing MG molecules from aqueous solutions, it is imperative to investigate the influence of adsorbent dosage. Generally, the adsorption capacity is inversely proportional to the adsorbent dosage because of the overlapping of readily available active sites for dye adsorption. Another possible explanation could be that a high adsorbent dosage leads to the unsaturation of adsorbent sites and enhances aggregation, thereby increasing the diffusion path length and decreasing the total surface area of the adsorbent. On the other hand, a greater adsorbent dosage increases the removal percentage of the dye due to the higher total surface area and the availability of more active sites ready for adsorption until the attainment of equilibrium (Bilal et al., 2022).

Baek et al. (2010a) quantified the adsorption percentage of MG using degreased coffee bean (DCB) at different adsorbent dosages with a fixed adsorbate concentration. Baek et al. (2010b) found that increasing the adsorbent dosage made many active sites available for a fixed MG concentration, enhancing adsorption. Abdi et al. (2017) studied the adsorption removal percentage of MG and the adsorption capacities of the zeolitic imidazolate framework (ZIF-8) and its hybrid nanocomposites based on graphene oxide (GO) and carbon nanotubes (CNTs) at different dosages. The adsorption of MG increased with the adsorbent dosage, whereas the adsorption capacities of all the three adsorbents decreased as the adsorbent dosage was increased. Of the three adsorbents, ZIF-8 was least efficient because of its inability to disperse during the sorption process. The developed hybrid nanocomposites enhanced the adsorptive surface area. The enhancement in surface area thereby resulted in more available active surface sites. However, ZIF-8@CNT-3 nanocomposites were an exception of this observation because their structure aggregated, leading to reduced surface area. The observed reduction in the surface area of ZIF-8@CNT-3 subsequently led to a decrease in the MG

removal percentage. Haounati et al. (2021) investigated MG removal using the SDS/CTAB@Montmorillonite organoclay composite. It was observed that the MG removal percentage increased from 73.26% to 99.32% when the adsorbent dosage was increased from 0.1 g/L to 1.0 g/L. This was attributed to more available sites at the adsorbent surface, leading to an increase of the contact surface area between MG dye and adsorbent surface. In contrast, the adsorbent capacity of MG by the SDS/CTAB@Montmorillonite organoclay composite decreased from 1 465.31 mg/g to 198.511 mg/g when the dosage was increased from 0.1 g/L to 1.0 g/L (Haounati et al., 2021). This significant decline could be attributed to the fact that a high adsorbent dosage is insufficient to combine with the active adsorption sites, resulting in a surface equilibrium state. Sharma and Nandi (2013) investigated the effect of sugarcane bagasse (SDP) dosage on the dye uptake and removal percentage of MG dye at different initial dye concentrations of 25 mg/L, 50 mg/L, 75 mg/L, and 100 mg/L. At each adsorbent dosage, MG adsorption potential increased with the adsorbate concentration. This was because the initial dye concentration provided more adsorption sites (Sharma and Nandi, 2013). All these studies suggest that it is necessary to determine the optimum dosage of the adsorbent in order to achieve the maximum removal efficiency for MG molecules.

3.3. Influence of initial MG concentration

The initial dye concentration significantly influences adsorption because it increases the ratio of dye molecules to the surface area of the adsorbent and improves the molecular diffusion of dyes into the adsorbent (Mehmandost et al., 2022). Due to the availability of more adsorption sites and functional groups on the adsorbent, the adsorption capacity increases with the initial dye concentration (Dutta et al., 2021). However, the adsorption capacity decreases because of the limited adsorbent surface area (Zhou et al., 2019). Yu et al. (2017) conducted a study on the MG uptake using CO_2-activated porous carbon derived from cattail biomass and reported an increase in the adsorption capacity from 93.24 mg/g to 210.18 mg/g as the initial concentration was increased from 40 mg/L to 100 mg/L. This was attributed to a strong driving force provided by the initial dye concentration to overpower the resistance to mass transfer of dyes between solid and aqueous phases. Likewise, the MG adsorption capacity of durian seed-based activated carbon increased from 22.00 mg/g to 332.08 mg/g when the initial MG concentration was increased from 25 mg/L to 500 mg/L. This was because of the availability of more active sites at the initial stage. Subsequently, the adsorption rate became slow because of the electrostatic repulsion between solute molecules and bulk phases of the adsorbent (Ahmad et al., 2014).

Furthermore, several studies have revealed that increasing the initial MG concentration resulted in a decrease in the MG removal percentage. This is attributed to the saturation of adsorption sites on the adsorbent surface caused by the adsorbate species. Peighambardoust et al. (2020) observed that the MG removal efficiency declined from 91.34% to 47.43% for carboxymethyl cellulose-g-polyacrylamide hydrogel and decreased from 94.914% to 51.460% for carboxymethyl cellulose-g-polyacrylamide/montmorillonite nanocomposite hydrogel. The active sites of the adsorbent became saturated, leading to an increasing electrostatic repulsion between the adsorbent surface and cationic MG dye molecules (Peighambardoust et al., 2020). Similarly, Deokar and Sabale (2014) examined the removal of methylene blue and MB from a binary solution on dried *Ulva lactuca* and found a decrease in the removal percentage of MG when the initial concentration of the binary solution was increased. This was due to the formation of a monolayer over the adsorbent surface at a low initial dye concentration.

4. Conclusions

Malachite green is a useful dye but becomes toxic to human when ingested through water. Sequel to the carcinogenic, mutagenic, and toxicity potentials of MG, the present synthesis comprehensively discusses two basic elimination strategies of MG from wastewater. Chemical methods have lower comparable merits to the adsorption technology, in terms of operational cost, sustainability, simplicity, resource availability, and operational expertise. Improvement of these techniques is needed to overcome their shortcomings because the yearning for clean water is still a continuous process.

Declaration of competing interest

The authors declare no conflicts of interest.

Acknowledgements

Peter Olusakin Oladoye would like to appreciate Prof. Yong Cai for providing laboratory space and enabling the environment for his doctoral research activities. Timothy Oladiran Ajiboye would like to seize this opportunity to gratefully appreciate Nelson Mandela University for the postdoctoral fundings and for providing laboratory space and enabling the environment for his postdoctoral research activities.

Appendix A. Supplementary data

Supplementary data to this article can be found online at https://doi.org/10.1016/j.wse.2023.03.002.

References

Abdi, J., Vossoughi, M., Mahmoodi, N.M., Alemzadeh, I., 2017. Synthesis of metal-organic framework hybrid nanocomposites based on GO and CNT with high adsorption capacity for dye removal. Chem. Eng. J. 326, 1145−1158. https://doi.org/10.1016/j.cej.2017.06.054.

Adebayo, M.A., Adebomi, J.I., Abe, T.O., Areo, F.I., 2020. Removal of aqueous Congo red and malachite green using ackee apple seed−bentonite

composite. Colloid Interf. Sci. Commun. 38, 100311. https://doi.org/10.1016/j.colcom.2020.100311.

Ahmad, A.L., Harris, W., Syafiie, S., Seng, O., 2002. Removal of dye from wastewater of textile industry using membrane technology. Jurnal Teknologi 36, 31−44. https://doi.org/10.11113/jt.v36.581.

Ahmad, M., Rajapaksha, A.U., Lim, J.E., Zhang, M., Bolan, N., Mohan, D., Vithanage, M., Lee, S.S., Ok, Y.S., 2014. Biochar as a sorbent for contaminant management in soil and water: A review. Chemosphere 99, 19−33. https://doi.org/10.1016/j.chemosphere.2013.10.071.

Ajiboye, T.O., Kuvarega, A.T., Onwudiwe, D.C., 2020. Recent strategies for environmental remediation of organochlorine pesticides. Appl. Sci. 10(18), 6286. https://doi.org/10.3390/app10186286.

Ajiboye, T.O., Oyewo, O.A., Onwudiwe, D.C., 2021a. Adsorption and photocatalytic removal of Rhodamine B from wastewater using carbon-based materials. FlatChem 29, 100277. https://doi.org/10.1016/j.flatc.2021.100277.

Ajiboye, T.O., Oyewo, O.A., Onwudiwe, D.C., 2021b. Photocatalytic removal of parabens and halogenated products in wastewater: A review. Environ. Chem. Lett. 19(5), 3789−3819. https://doi.org/10.1007/s10311-021-01263-2.

Ajiboye, T.O., Oyewo, O.A., Onwudiwe, D.C., 2021c. Simultaneous removal of organics and heavy metals from industrial wastewater: A review. Chemosphere 262, 128379. https://doi.org/10.1016/j.chemosphere.2020.128379.

Allègre, C., Moulin, P., Maisseu, M., Charbit, F., 2006. Treatment and reuse of reactive dyeing effluents. J. Membr. Sci. 269(1), 15−34. https://doi.org/10.1016/j.memsci.2005.06.014.

Amigun, A.T., Adekola, F.A., Tijani, J.O., Mustapha, S., 2022. Photocatalytic degradation of malachite green dye using nitrogen/sodium/iron-TiO_2 nanocatalysts. Results in Chemistry 4, 100480. https://doi.org/10.1016/j.rechem.2022.100480.

Amuda, O., Giwa, A., Bello, I., 2007. Removal of heavy metal from industrial wastewater using modified activated coconut shell carbon. Biochem. Eng. J. 36(2), 174−181. https://doi.org/10.1016/j.bej.2007.02.013.

Awokoya, K.N., Oninla, V.O., Adeyinka, G.C., Ajadi, M.O., Chidimma, O.T., Fakola, E.G., Akinyele, O.F., 2022. Experimental and computational studies of microwave-assisted watermelon rind − styrene based molecular imprinted polymer for the removal of malachite green from aqueous solution. Sci. Africa. 16, e01194. https://doi.org/10.1016/j.sciaf.2022.e01194.

Baek, M.-H., Ijagbemi, C.O., Kim, D.-S., 2010a. Spectroscopic studies on the oxidative decomposition of Malachite Green using ozone. J. Env. Sci. Health A 45(5), 630−636. https://doi.org/10.1080/10934521003595779.

Baek, M.-H., Ijagbemi, C.O., Se-Jin, O., Kim, D.-S., 2010b. Removal of Malachite Green from aqueous solution using degreased coffee bean. J. Hazard Mater. 176(1−3), 820−828. https://doi.org/10.1016/j.jhazmat.2009.11.110.

Bai, C., Xiao, W., Feng, D., Xian, M., Guo, D., Ge, Z., Zhou, Y., 2013. Efficient decolorization of Malachite Green in the Fenton reaction catalyzed by [Fe(III)-salen]Cl complex. Chem. Eng. J. 215−216, 227−234. https://doi.org/10.1016/j.cej.2012.09.124.

Bharati, B., Sonkar, A., Singh, N., Dash, D., Rath, C., 2017. Enhanced photocatalytic degradation of dyes under sunlight using biocompatible TiO_2 nanoparticles. Mater. Res. Express 4(8). https://doi.org/10.1088/2053-1591/aa6a36, 085503.

Bilal, M., Ihsanullah, I., Shah, M.U.H., Reddy, A.V.B., Aminabhavi, T.M., 2022. Recent advances in the removal of dyes from wastewater using low-cost adsorbents. J. Environ. Manag. 321, 115981. https://doi.org/10.1016/j.jenvman.2022.115981.

Buvaneswari, K., Singanan, M., 2022. Removal of malachite green dye in synthetic wastewater using *zingiber officinale* plant leaves biocarbon. Mater. Today Proc. 55, 274−279. https://doi.org/10.1016/j.matpr.2021.07.137.

Chaplin-Kramer, R., Sharp, R.P., Weil, C., Bennett, E.M., Pascual, U., Arkema, K.K., Brauman, K.A., Bryant, B.P., Guerry, A.D., Haddad, N.M., 2019. Global modeling of nature's contributions to people. Science 366(6462), 255−258. https://doi.org/10.1126/science.aaw3372.

Chen, C., Lu, C., Chung, Y., Jan, J., 2007. UV light induced photodegradation of malachite green on TiO_2 nanoparticles. J. Hazard. Mater. 141(3), 520−528. https://doi.org/10.1016/j.jhazmat.2006.07.011.

Chen, F., Ma, W., He, J., Zhao, J., 2002. Fenton degradation of malachite green catalyzed by aromatic additives. J. Phys. Chem. 106(41), 9485−9490. https://doi.org/10.1021/jp0144350.

Cheng, C., Liang, Q., Yan, M., Liu, Z., He, Q., Wu, T., Luo, S., Pan, Y., Zhao, C., Liu, Y., 2022. Advances in preparation, mechanism and applications of graphene quantum dots/semiconductor composite photocatalysts: A review. J. Hazard Mater. 424, 127721. https://doi.org/10.1016/j.jhazmat.2021.127721.

Culp, S., Beland, F., Heflich, R., Benson, R., Blankenship, L., Webb, P., Mellick, P., Trotter, R., Shelton, S., Greenlees, K.J., et al., 2002. Mutagenicity and carcinogenicity in relation to DNA adduct formation in rats fed leucomalachite green. Mutat. Res. Fund. Mol. Mech. Mutagen. 506(507), 55−63. https://doi.org/10.1016/S0027-5107(02)00152-5.

Deokar, R., Sabale, A., 2014. Biosorption of methylene blue and malachite green from binary solution onto *Ulva lactuca*. Int. J. Curr. Microbiol. Appl. Sci. 3(5), 295−304.

Dihom, H.R., Al-Shaibani, M.M., Mohamed, R.M.S.R., Al-Gheethi, A.A., Sharma, A., Khamidun, M.H.B., 2022. Photocatalytic degradation of disperse azo dyes in textile wastewater using green zinc oxide nanoparticles synthesized in plant extract: A critical review. J. Water Process Eng. 47, 102705. https://doi.org/10.1016/j.jwpe.2022.102705.

Dutta, S., Gupta, B., Srivastava, S.K., Gupta, A.K., 2021. Recent advances on the removal of dyes from wastewater using various adsorbents: A critical review. Materials Advances 2(14), 4497−4531. https://doi.org/10.1039/D1MA00354B.

El-Kady, A.A., Wade, T.L., Sweet, S.T., 2018. Assessment and ecological indicators of total and polycyclic aromatic hydrocarbons in the aquatic environment of lake Manzala, Egypt. J. Env. Sci. Health A. 53(9), 854−865. https://doi.org/10.1080/10934529.2018.1455376.

García-Rodríguez, O., Bañuelos, J.A., El-Ghenymy, A., Godínez, L.A., Brillas, E., Rodríguez-Valadez, F.J., 2016. Use of a carbon felt−iron oxide air-diffusion cathode for the mineralization of Malachite Green dye by heterogeneous electro-Fenton and UVA photoelectro-Fenton processes. J. Electroanal. Chem. 767, 40−48. https://doi.org/10.1016/j.jelechem.2016.01.035.

Ghime, D., Goru, P., Ojha, S., Ghosh, P., 2019. Oxidative decolorization of a malachite green oxalate dye through the photochemical advanced oxidation processes. Global NEST Journal 21(2), 195−203. https://doi.org/10.30955/gnj.003000.

Ghodbane, H., Hamdaoui, O., 2010. Decolorization of antraquinonic dye, C.I. Acid Blue 25, in aqueous solution by direct UV irradiation, UV/H_2O_2 and UV/Fe(II) processes. Chem. Eng. J. 160(1), 226−231. https://doi.org/10.1016/j.cej.2010.03.049.

Giang, N.T.H., Hai, N.D., Thinh, N.T., Tan, N.N., Phuong, L.P., Thinh, D.B., Van Duc, N., Viet, V.N.D., Duy, H.K., Phong, M.T., et al., 2022. Enhanced photocatalytic degradation of malachite green by sulfur-doped titanium dioxide/porous reduced graphene oxide. Diam. Relat. Mater. 129, 109321. https://doi.org/10.1016/j.diamond.2022.109321.

Gündüz, F., Bayrak, B., 2017. Biosorption of malachite green from an aqueous solution using pomegranate peel: Equilibrium modelling, kinetic and thermodynamic studies. J. Mol. Liq. 243, 790−798. https://doi.org/10.1016/j.molliq.2017.08.095.

Hameed, B.H., Lee, T.W., 2009. Degradation of malachite green in aqueous solution by Fenton process. J. Hazard. Mater. 164(2−3), 468−472. https://doi.org/10.1016/j.jhazmat.2008.08.018.

Haounati, R., El Guerdaoui, A., Ouachtak, H., El Haouti, R., Bouddouch, A., Hafid, N., Bakiz, B., Santos, D., Taha, M.L., Jada, A., 2021. Design of direct Z-scheme superb magnetic nanocomposite photocatalyst Fe_3O_4/Ag_3PO_4@ Sep for hazardous dye degradation. Separ. Purif. Technol. 277, 119399. https://doi.org/10.1016/j.seppur.2021.119399.

Hashemian, S., 2013. Fenton-like oxidation of malachite green solutions: Kinetic and thermodynamic study. J. Chem. 2013, 809318. https://doi.org/10.1155/2013/809318.

Ho, S., 2020. Removal of dyes from wastewater by adsorption onto activated carbon: Mini review. J. Geosci. Environ. Protect. 8(5), 100280. https://doi.org/10.4236/gep.2020.85008.

Hubbs, A., Porter, D.W., Mercer, R., Castranova, V., Sargent, L., Sriram, K., 2013. Chapter 43 - Nanoparticulates. In: Haschek, W.M., Rousseaux, C.G., Wallig, M.A. (Eds.), Haschek and Rousseaux's Handbook of Toxicologic Pathology, Third Edition. Academic Press, Pittsburgh, pp. 1373−1419. https://doi.org/10.1016/B978-0-12-415759-0.00043-1.

Iqbal, A., Cevik, E., Bozkurt, A., Asiri, S.M.M., Alagha, O., Qahtan, T.F., Jalees, M.I., Farooq, M.U., 2022. Ultrahigh adsorption by regenerable iron-cobalt core-shell nanospheres and their synergetic effect on nano-hybrid membranes for removal of malachite green dye. J. Environ. Chem. Eng. 10(3), 107968. https://doi.org/10.1016/j.jece.2022.107968.

Jaffari, Z.H., Abbas, A., Lam, S.-M., Park, S., Chon, K., Kim, E.-S., Cho, K.H., 2022. Machine learning approaches to predict the photocatalytic performance of bismuth ferrite-based materials in the removal of malachite green. J. Hazard. Mater. 442, 130031. https://doi.org/10.1016/j.jhazmat.2022.130031.

Jiang, D.B., Liu, X., Xu, X., Zhang, Y.X., 2018. Double-shell Fe_2O_3 hollow box-like structure for enhanced photo-Fenton degradation of malachite green dye. J. Phys. Chem. Solid. 112, 209−215. https://doi.org/10.1016/j.jpcs.2017.09.033.

Karimi, A., Aghbolaghy, M., Khataee, A., Bargh, S., 2012. Use of enzymatic bio-Fenton as a new approach in decolorization of malachite green. Sci. World J. 2012, 1−6.

Khan, J.A., He, X., Khan, H.M., Shah, N.S., Dionysiou, D.D., 2013. Oxidative degradation of atrazine in aqueous solution by $UV/H_2O_2/Fe^{2+}$, $UV/S_2O_8^{2-}/Fe^{2+}$ and $UV/HSO_5^-/Fe^{2+}$ processes: A comparative study. Chemical Engineering Journal 218, 376−383. https://doi.org/10.1016/j.cej.2012.12.055.

Kishor, R., Purchase, D., Saratale, G.D., Saratale, R.G., Ferreira, L.F.R., Bilal, M., Chandra, R., Bharagava, R.N., 2021. Ecotoxicological and health concerns of persistent coloring pollutants of textile industry wastewater and treatment approaches for environmental safety. J. Environ. Chem. Eng. 9(2), 105012. https://doi.org/10.1016/j.jece.2020.105012.

Kumar, P., Agnihotri, R., Wasewar, K., Uslu, H., Yoo, C., 2012. Status of adsorptive removal of dye from textile industry effluent. Desalination Water Treat. 50, 226−244. https://doi.org/10.1080/19443994.2012.719472.

Lee, Y.-C., Kim, E.J., Yang, J.-W., Shin, H.-J., 2011. Removal of malachite green by adsorption and precipitation using aminopropyl functionalized magnesium phyllosilicate. J. Hazard. Mater. 192(1), 62−70. https://doi.org/10.1016/j.jhazmat.2011.04.094.

Lellis, B., Fávaro-Polonio, C.Z., Pamphile, J.A., Polonio, J.C., 2019. Effects of textile dyes on health and the environment and bioremediation potential of living organisms. Biotechnol. Res. Innov. 3(2), 275−290. https://doi.org/10.1016/j.biori.2019.09.001.

Li, H.J., Xu, J.H., Wang, L.Q., Hou, D.D., Wang, Z.R., Li, H.Z., 2022. Adsorption properties of modified ATP-RGO composite aerogel for removal of malachite green and methyl orange from initary and binary aqueous solutions. Adsorpt. Sci. Technol. 2022, 5455330. https://doi.org/10.1155/2022/5455330.

Marszałek, J., Żyłła, R., 2021. Recovery of water from textile dyeing using membrane filtration processes. Processes 9(10), 1833. https://doi.org/10.3390/pr9101833.

Mazloom, F., Masjedi-Arani, M., Ghiyasiyan-Arani, M., Salavati-Niasari, M., 2016. Novel sodium dodecyl sulfate-assisted synthesis of $Zn_3V_2O_8$ nanostructures via a simple route. J. Mol. Liq. 214, 46−53. https://doi.org/10.1016/j.molliq.2015.11.033.

Mehmandost, N., Goudarzi, N., Chamjangali, M.A., Bagherian, G., 2022. Application of random forest for modeling batch and continuous fixed-bed removal of crystal violet from aqueous solutions using Gypsophila aretioides stem-based biosorbent. Spectrochim. Acta Mol. Biomol. Spectrosc. 265, 120292. https://doi.org/10.1016/j.saa.2021.120292.

Modirshahla, N., Behnajady, M.A., 2006. Photooxidative degradation of Malachite Green (MG) by UV/H_2O_2: Influence of operational parameters and kinetic modeling. Dyes Pigments 70(1), 54−59. https://doi.org/10.1016/j.dyepig.2005.04.012.

Mohamed Shameer, P., Mohamed Nishath, P., 2019. Chapter 8 - Exploration and enhancement on fuel stability of biodiesel: A step forward in the track of global commercialization. In: Azad, A.K., Rasul, M. (Eds.), Woodhead Publishing Series in Energy, Advanced Biofuels. Woodhead Publishing, Sawston, pp. 181−213. https://doi.org/10.1016/B978-0-08-102791-2.00008-8.

Moradi, O., Panahandeh, S., 2022. Fabrication of different adsorbents based on zirconium oxide, graphene oxide, and dextrin for removal of green malachite dye from aqueous solutions. Environ. Res. 214, 114042. https://doi.org/10.1016/j.envres.2022.114042.

Naushad, M., Alqadami, A.A., Al-Kahtani, A.A., Ahamad, T., Awual, M.R., Tatarchuk, T., 2019. Adsorption of textile dye using para-aminobenzoic acid modified activated carbon: Kinetic and equilibrium studies. J. Mol. Liq. 296, 112075. https://doi.org/10.1016/j.molliq.2019.112075.

Navarro, P., Zapata, J.P., Gotor, G., Gonzalez-Olmos, R., Gómez-López, V.M., 2019. Degradation of malachite green by a pulsed light/H_2O_2 process. Water Sci. Technol. 79(2), 260−269. https://doi.org/10.2166/wst.2019.041.

Ojediran, J.O., Dada, A.O., Aniyi, S.O., David, R.O., Adewumi, A.D., 2021. Mechanism and isotherm modeling of effective adsorption of malachite green as endocrine disruptive dye using Acid Functionalized Maize Cob (AFMC). Sci. Rep. 11(1), 21498. https://doi.org/10.1038/s41598-021-00993-1.

Oladoye, P.O., 2022. Natural, low-cost adsorbents for toxic Pb(II) ion sequestration from (waste) water: A state-of-the-art review. Chemosphere 287, 132130. https://doi.org/10.1016/j.chemosphere.2021.132130.

Oladoye, P.O., Bamigboye, O.M., Ogunbiyi, O.D., Akano, M.T., 2022. Toxicity and decontamination strategies of Congo red dye. Groundwater Sustain. Dev. 19, 100844. https://doi.org/10.1016/j.gsd.2022.100844.

Oplatowska, M., Donnelly, R.F., Majithiya, R.J., Kennedy, D.G., Elliott, C.T., 2011. The potential for human exposure, direct and indirect, to the suspected carcinogenic triphenylmethane dye Brilliant Green from green paper towels. Food Chem. Toxicol. 49(8), 1870−1876. https://doi.org/10.1016/j.fct.2011.05.005.

Oturan, M.A., Guivarch, E., Oturan, N., Sirés, I., 2008. Oxidation pathways of malachite green by Fe^{3+}-catalyzed electro-Fenton process. Appl. Catal. B Environ. 82(3−4), 244−254. https://doi.org/10.1016/j.apcatb.2008.01.016.

Pandey, D., Daverey, A., Dutta, K., Arunachalam, K., 2022. Bioremoval of toxic malachite green from water through simultaneous decolorization and degradation using laccase immobilized biochar. Chemosphere 297, 134126. https://doi.org/10.1016/j.chemosphere.2022.134126.

Patel, M., Surti, M., Siddiqui, A.J., Adnan, M., 2021. Chapter 27 - Fungi and metal nanoparticles. In: Kharisov, B., Kharissova, O. (Eds.), Handbook of Greener Synthesis of Nanomaterials and Compounds. Elsevier, Amsterdam, pp. 861−890. https://doi.org/10.1016/B978-0-12-821938-6.00027-X.

Pathy, A., Krishnamoorthy, N., Chang, S.X., Paramasivan, B., 2022. Malachite green removal using algal biochar and its composites with kombucha SCOBY: An integrated biosorption and phycoremediation approach. Surface. Interfac. 30, 101880. https://doi.org/10.1016/j.surfin.2022.101880.

Peighambardoust, S.J., Aghamohammadi-Bavil, O., Foroutan, R., Arsalani, N., 2020. Removal of malachite green using carboxymethyl cellulose-g-polyacrylamide/montmorillonite nanocomposite hydrogel. Int. J. Biol. Macromol. 159, 1122−1131. https://doi.org/10.1016/j.ijbiomac.2020.05.093.

Ramaraju, B., Manoj Kumar Reddy, P., Subrahmanyam, C., 2014. Low cost adsorbents from agricultural waste for removal of dyes. Environ. Prog. Sustain. Energy 33(1), 38−46. https://doi.org/10.1002/ep.11742.

Raval, A.R., Kohli, H.P., Mahadwad, O.K., 2022. Application of emulsion liquid membrane for removal of malachite green dye from aqueous solution: Extraction and stability studies. Chem. Eng. J. Adv. 12, 100398. https://doi.org/10.1016/j.ceja.2022.100398.

Samuchiwal, S., Gola, D., Malik, A., 2021. Decolourization of textile effluent using native microbial consortium enriched from textile industry effluent. J. Hazard. Mater. 402, 123835. https://doi.org/10.1016/j.jhazmat.2020.123835.

Sasmal, D., Banerjee, S., Senapati, S., Tripathy, T., 2020. Effective removal of Th^{4+}, Pb^{2+}, Cd^{2+}, malachite green, methyl violet and methylene blue from their aqueous solution by amylopectin dialdehyde-Schiff base. J. Environ. Chem. Eng. 8(3), 103741. https://doi.org/10.1016/j.jece.2020.103741.

Scott, K., Hughes, R., Hughes, R., 1996. Industrial Membrane Separation Technology. Springer, Berlin.

Seliem, M.K., Barczak, M., Anastopoulos, I., Giannakoudakis, D.A., 2020. A novel nanocomposite of activated serpentine mineral decorated with

magnetic nanoparticles for rapid and effective adsorption of hazardous cationic dyes: Kinetics and equilibrium studies. Nanomaterials 10(4), 684. https://doi.org/10.3390/nano10040684.

Sghaier, I., Guembri, M., Chouchane, H., Mosbah, A., Ouzari, H.I., Jaouani, A., Cherif, A., Neifar, M., 2019. Recent advances in textile wastewater treatment using microbial consortia. J. Text. Eng. Fash. Technol. 5(3), 134−146. https://doi.org/10.15406/jteft.2019.05.00194.

Sharma, N., Nandi, B.K., 2013. Utilization of sugarcane baggase, an agricultural waste to remove malachite green dye from aqueous solutions. J. Mater. Environ. Sci. 4(6), 1052−1065.

Shi, Z., Xu, C., Guan, H., Li, L., Fan, L., Wang, Y., Liu, L., Meng, Q., Zhang, R., 2018. Magnetic metal organic frameworks (MOFs) composite for removal of lead and malachite green in wastewater. Colloids Surf. A Physicochem. Eng. Asp. 539, 382−390. https://doi.org/10.1016/j.colsurfa.2017.12.043.

Shrivastava, V., Ali, I., Marjub, M.M., Rene, E.R., Soto, A.M.F., 2022. Wastewater in the food industry: Treatment technologies and reuse potential. Chemosphere 293, 133553. https://doi.org/10.1016/j.chemosphere.2022.133553.

Singh, P., Raizada, P., Kumari, S., Kumar, A., Pathania, D., Thakur, P., 2014. Solar-Fenton removal of malachite green with novel Fe^0-activated carbon nanocomposite. Appl. Catal. Gen. 476, 9−18. https://doi.org/10.1016/j.apcata.2014.02.009.

Sleeman, R., Carter, J.F., 2005. Forensic sciences | Explosives. In: Worsfold, P., Townshend, P., Poole, C. (Eds.), Encyclopedia of Analytical Science, Second Edition. Elsevier, Amsterdam, pp. 400−406. https://doi.org/10.1016/B0-12-369397-7/00198-9.

Song, J., Han, G., Wang, Y., Jiang, X., Zhao, D., Li, M., Yang, Z., Ma, Q., Parales, R.E., Ruan, Z., 2020. Pathway and kinetics of malachite green biodegradation by *Pseudomonas veronii*. Sci. Rep. 10, 4502. https://doi.org/10.1038/s41598-020-61442-z.

Srivastava, S., Sinha, R., Roy, D., 2004. Toxicological effects of malachite green. Aquat. Toxicol. 66(3), 319−329. https://doi.org/10.1016/j.aquatox.2003.09.008.

Tran, T.V., Nguyen, D.T.C., Kumar, P.S., Din, A.T.M., Qazaq, A.S., Vo, D.V.N., 2022. Green synthesis of Mn_3O_4 nanoparticles using *Costus woodsonii* flowers extract for effective removal of malachite green dye. Environ. Res. 214, 113925. https://doi.org/10.1016/j.envres.2022.113925.

Tsai, C.-Y., Lin, P.-Y., Hsieh, S.-L., Kirankumar, R., Patel, A.K., Singhania, R.-R., Dong, C.-D., Chen, C.-W., Hsieh, S., 2022. Engineered mesoporous biochar derived from rice husk for efficient removal of malachite green from wastewaters. Bioresour. Technol. 347, 126749. https://doi.org/10.1016/j.biortech.2022.126749.

World Health Organization (WHO), 2017. Progress on Drinking Water, Sanitation and Hygiene: 2017 Update and SDG Baselines. WHO, Geneva.

Wu, J., Yang, J., Feng, P., Wen, L., Huang, G., Xu, C., Lin, B., 2022. Highly efficient and ultra-rapid adsorption of malachite green by recyclable crab shell biochar. J. Ind. Eng. Chem. 113, 206−214. https://doi.org/10.1016/j.jiec.2022.05.047.

Young, S.L., Boateng, G.O., Jamaluddine, Z., Miller, J.D., Frongillo, E.A., Neilands, T.B., Collins, S.M., Wutich, A., Jepson, W.E., Stoler, J., 2019. The Household Water InSecurity Experiences (HWISE) Scale: Development and validation of a household water insecurity measure for low-income and middle-income countries. BMJ Global Health 4(5), e001750. https://doi.org/10.1136/bmjgh-2019-001750.

Yu, M., Han, Y., Li, J., Wang, L., 2017. CO_2-activated porous carbon derived from cattail biomass for removal of malachite green dye and application as supercapacitors. Chem. Eng. J. 317, 493−502. https://doi.org/10.1016/j.cej.2017.02.105.

Zhang, P., Hou, D., O'Connor, D., Li, X., Pehkonen, S., Varma, R.S., Wang, X., 2018. Green and size-specific synthesis of stable Fe−Cu oxides as earth-abundant adsorbents for Malachite green removal. ACS Sustain. Chem. Eng. 6(7), 9229−9236. https://doi.org/10.1021/acssuschemeng.8b0154.7.

Zhao, J., Liu, X., 2022. Electron microscopic methods (TEM, SEM and energy dispersal spectroscopy). In: Reference Module in Earth Systems and Environmental Sciences. Elsevier, Amsterdam. https://doi.org/10.1016/B978-0-12-822974-3.00013-6.

Zhou, Z., Liu, X., Sun, K., Lin, C., Ma, J., He, M., Ouyang, W., 2019. Persulfate-based advanced oxidation processes (AOPs) for organic-contaminated soil remediation: A review. Chem. Eng. J. 372, 836−851. https://doi.org/10.1016/j.cej.2019.04.213.